Anomalous enhancement of ionospheric F_2 layer critical frequency and total electron content over low latitudes before three recent major earthquakes in China

Kavita Sharma,[1] R. S. Dabas,[1] S. K. Sarkar,[1] R. M. Das,[1] Sudha Ravindran,[2] and A. K. Gwal[3]

[1] This paper reports unusual variations in the ionospheric total electron content (TEC) and the critical frequency of the F_2 layer (foF_2) a few days before the main shock of three major earthquakes ($M > 6$). Epicenters of these earthquakes are distributed in China. Ionospheric data, recorded by an Indian network of ionosonde and GPS receivers at Delhi (28.6°N, 77.2°E), Bhopal (23.29°N, 77.46°E), and Trivandrum (8.4°N, 76.6°E) are analyzed to find seismoionospheric signatures of three recent major earthquakes in China. The results clearly indicate large enhancements in foF_2 and TEC on geomagnetic quiet days, observed mainly at a low-latitude station in Delhi, which is nearest to the earthquake epicenters. The anomalous behavior of foF_2 and TEC appeared 1–4 days before the main shock and especially during 1100–1700 LT. However, the ionospheric foF_2 and TEC variability at the equatorial station Trivandrum and equatorial anomaly station Bhopal did not show any significant changes, thereby indicating the localized nature of such unusual ionospheric variations. The observed results suggest that the unusual enhancements of ionospheric foF_2 and TEC over Delhi a few days before the main shock of each earthquake are most likely due to a seismoionospheric link.

Citation: Sharma, K., R. S. Dabas, S. K. Sarkar, R. M. Das, S. Ravindran, and A. K. Gwal (2010), Anomalous enhancement of ionospheric F_2 layer critical frequency and total electron content over low latitudes before three recent major earthquakes in China,

1. Introduction

[2] In recent years, coupling between the dynamics of lithospheric processes and ionospheric anomalies prior to earthquakes is of growing interest. Both ground-based ionosonde observations [*Ondoh and Hayakawa*, 1999; *Liu et al.*, 2000; *Chuo et al.*, 2002; *Popov et al.*, 2004; *Liperovskaya et al.*, 2006; *Dabas et al.*, 2007; *Dutta et al.*, 2007; *Sharma et al.*, 2008] and topside sounding observations [*Gokhberg et al.*, 1983; *Pulinets and Legen'ka*, 2003] have shown that ionospheric variations associated with seismic activity do exist, and appear as precursory effects a few days to a few weeks before an earthquake of large intensity ($M > 6$). A wide class of ionospheric anomalies can be observed in plasma density, temperature, and composition. A number of space-plasma parameters exist, with seismic-related variations of electron density "NmF_2" at the ionospheric F layer peak among the most sensitive parameters. NmF_2 can be measured by a vertical sounding method either by a ground-based ionosonde network or from satellites. Another important parameter, total electron content (TEC), is also widely used to examine the effects of seismic activity on ionospheric variations. Researchers have reported observations of seismoionospheric variations with both positive (enhancement) and negative (depletion) effects on electron density [*Pulinets et al.*, 1994; *Zelenova and Legen'ka*, 1988; *Zelenova et al.*, 1991; *Ishkova et al.*, 1994; *Legen'ka et al.*, 1995]. No regularity in sign changes for the seismoionospheric variations has been found yet. However, previous reports of seismoionospheric variations over Delhi were dominantly positive electron density changes. *Pulinets and Boyarchuk* [2004] summarized the major characteristics of the observed ionospheric anomalies based on hundreds of seismic cases processed using ground-based and satellite measurements. *Liu et al.* [2004] suggested the presence of temporal characteristics with 5 day intervals in ionospheric precursors after processing continuous global positioning system (GPS) TEC data for 20 strong earthquakes ($M \geq 6$) in the Taiwan area. They also reported that the most sensitive pre-earthquake feature appeared to be the negative ionospheric anomalies within the 1800–2200 LT sector. Spatial distribution of ionospheric precursors can be obtained by combining data from topside sounding and ground-based ionospheric stations as well as from GPS networks [*Liu et al.*, 2001; *Pulinets and*

Table 1. Main Parameters of Three Major 2008 Earthquakes in China

Earthquake Epicenter	Date	Time of Main Shock (LT)	Location: Latitude (°N)	Location: Longitude (°E)	M	Depth (km)
Xinjiang-Xizang Border Region, China	20 Mar 2008	0403:01	35.49	81.39	7.2	22.9
Wenchuan County, China	12 May 2008	1158:01	31.0	103.4	8.0	19.0
Western Xizang, China	25 Aug 2008	0651:59	30.89	83.61	6.7	18

Legen'ka, 2003]. An advantage of satellite measurement is the possibility of obtaining a spatial and time dependent picture of the disturbed region. Previous studies show that the maximum extent of the affected area in the ionosphere does not coincide with the vertical projection of the epicenter of the future earthquake and shifts equatorward in high and middle latitudes. Also, an ionospheric anomaly over a seismically active area in one hemisphere can be mapped through geomagnetic field lines in the magnetically conjugated area of the opposite hemisphere [*Pulinets and Boyarchuk*, 2004]. *Pulinets et al.* [2000], using a quasi-electrostatic coupled model of the atmosphere-thermosphere-ionosphere reproduced the spatial distribution of ionospheric precursors. According to that study, the seismoionospheric anomalies appear as bifocal structures with the focus of the positive and negative perturbations of the maximum F_2 layer plasma concentration (NmF_2) on alternate sides of the epicenter.

[3] The ionosphere has large day-to-day variability due to solar radiation variability, geomagnetic influences, and solar wind energy input [*Rishbeth and Mendillo*, 2001]. Moreover, even at quiet geomagnetic activity levels, the ionosphere may have huge day-to-day variability due to geomagnetic activities as well as due to sources in the atmosphere or from below [*Liu et al.*, 2008a, 2008b]. In equatorial and low latitudes, the day-to-day distribution of ionospheric plasma is mainly controlled by $E \times B$ drifts and its latitudinal expansion depends upon solar and magnetic activity conditions. Therefore, it is difficult to distinguish the effects of earthquakes from other effects on ionospheric variability at these latitudes.

[4] In 2008, three major earthquakes ($M > 6$) struck China during the months of March, May, and August. This paper describes the anomalous ionospheric variations in foF_2 and GPS TEC recorded by a network of ionosondes and GPS receivers, respectively, a few days before the actual occurrence of these earthquakes. After statistically filtering the ionospheric variability in foF_2 and TEC, the temporal and spatial signatures of the anomalous ionospheric variations seem to be induced by the devastating earthquakes. The possible causes for these significant enhancements in ionospheric parameters are discussed.

2. Characteristics of Earthquakes

[5] The main parameters of the three earthquakes in the present analysis are listed in Table 1. Table 2 lists the radius of the earthquake preparation zone for each of the earthquakes, derived using the $\rho = 10^{0.43M}$ formula of *Dobrovolsky et al.* [1979] in which ρ is the radius of the earthquake preparation zone in km, and M, the magnitude of the earthquake on the Richter scale. Table 2 also contains information about distances of the ionospheric observing sites from the three epicenters. As seen in table 2, Delhi lies within the radius of the earthquake preparation zone for all three events. However, Bhopal (an equatorial ionization anomaly station in the Indian zone) lies only in the earthquake preparation zone for the Wenchuan earthquake of 12 May 2008, the strongest earthquake.

3. Data Set and Analysis Technique

[6] The present study is based on digital ionosonde observations at 15 minute intervals from Delhi, Bhopal, and Trivandrum (an equatorial station in the Indian zone) to examine the ionospheric variability over low latitudes around the period of earthquakes. *Liu et al.* [2004] developed a statistical method to segregate anomalous variability from day-to-day variability of the ionosphere. According to their method, an interquartile range (IQR) is calculated to construct and upper bound $X +$ IQR and a lower bound $X -$ IQR for data estimation, where X is the monthly median. Under the assumption of a normal distribution with mean m and standard deviation σ for the GPS TEC, the expected value of IQR is 1.34 σ. To produce a stringent criterion, the upper and lower bounds of IQR are calculated using

$$\text{IQR upper bound} = X(MM) + 1.34\ \sigma \tag{1}$$

$$\text{IQR lower bound} = X(MM) - 1.34\ \sigma, \tag{2}$$

where X and $\langle\sigma\rangle$ are the monthly median values of foF_2 and the standard deviation, respectively. Simultaneously, the variations are studied in more detail by calculating percentage increases and decreases from the IQR upper and lower bounds using

$$\%\ \text{Increase} = (foF_2 - \text{IQR upper bound}/\text{IQR upper bound}) \times 100, \tag{3}$$

Table 2. Radius of Earthquake Preparatory Zone and Effects of Three 2008 Major Earthquakes in China

Earthquake Epicenter	Radius of Earthquake Preparation Zone (km)	Distance (km) From: Delhi	Distance (km) From: Bhopal	Distance (km) From: Trivandrum	Main Precursor Occurrence	Effect on F_2 Layer Electron Density
Xinjiang-Xizang Border Region, China	1247	962[a]	1421	3132	1 d prior to main shock	Increased
Wenchuan County, China	2754	2533[a]	2630[a]	3778	2 d prior	Increased
Western Xizang, China	760	669[a]	1082	2725	3 d prior	Increased

[a]The observing sites within the Earthquake preparatory zone.

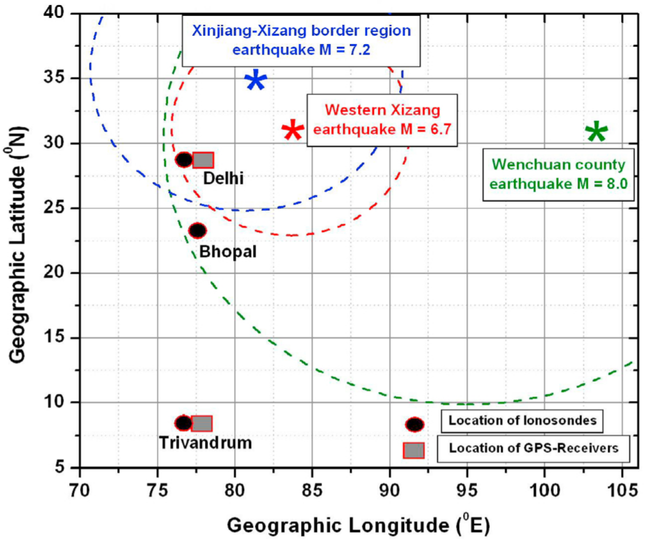

Figure 1. Geographic locations of three earthquake epicenters and ionospheric monitoring instruments (ionosondes and GPS receivers). Red stars indicate earthquake epicenters. Red, blue, and green circles with dashed lines represent the radius of the earthquake preparation zones for western Xizang, Xinjiang-Xizang border region, and Wenchuan County earthquakes, respectively.

where if foF_2 < IQR upper bound, then % Increase = 0, and

$$\% \text{ Decrease} = (\text{IQR lower bound} - foF_2/\text{IQR lower bound}) \times 100, \qquad (4)$$

where if IQR lower bound < foF_2, then % Increase = 0.

[7] It is to be pointed out here that although the above equations are generally used to remove the effects of day-to-day variability in the ionospheric data, the level of quiet-time variability may be different at different locations (e.g., Delhi, Bhopal, and Trivandrum); hence, the same criteria for all three stations may not always be appropriate.

[8] In addition to ionosonde data, TEC data obtained from a network of GPS receivers at Delhi and Trivandrum have also been used to examine the spatial distribution of ionospheric variability in the disturbed region. Figure 1 is a schematic representation of the epicenters and the locations of the ionosondes and the GPS receivers. GSV 4004B Ionospheric Scintillation and TEC Monitor receivers (GISTM) collect slant TEC data [*Van Dierendonck et al.*, 1996]. Such slant TEC data are collected at 1 minute intervals from both stations. Each GISTM can track up to 11 GPS *C*/*A* code signals at the *L*1 and *L*2 frequencies of 1.575 GHz and 1.2 GHz, respectively. A NovAtel Millennium dual frequency *L*1/*L*2 GPS Card is used to measure the pseudorange at *L*1 (1575.42 MHz), the carrier-to-noise ratio (C/N), and the phase advance at *L*1 and *L*2 (1227.60 MHz). The obtained slant TEC measurements are proportional to the ionospheric delay between *L*1 and *L*2 signals as

$$\mathrm{STEC} = \left[9.483 \times \left\{PR_{L2} - PR_{L1} - \Delta_{\frac{C}{A}-P,PRN}\right\} + \mathrm{TEC_{RX}} + \mathrm{TEC_{CAL}}\right] \mathrm{TEC}U, \qquad (5)$$

where PR_{L2} is the $L2$ pseudorange in meters, PR_{L1} is the $L1$ pseudorange in meters, $\Delta_{C/A-P,PRN}$ is the input bias between *SV C*/*A*- and *P*-code code-chip transitions in meters, $\mathrm{TEC_{RX}}$ is the TEC result due to internal receiver $L1/L2$ delay, $\mathrm{TEC_{CAL}}$ is the user defined TEC offset and 1 TECU = 10^{16} electrons/m^2.

[9] The measured slant TEC is corrected for the receiver differential delay $\mathrm{TEC_{CAL}}$. In equation (5), $\mathrm{TEC_{CAL}}$ represents the bias error corrections and is different for different satellite-receiver pairs and is updated from time to time. In the present study, the receiver part of the above bias is corrected by taking the value of −61.1484 TECU supplied by the manufacturer by calibrating the receiver against the Wide Area Augmentation System (WAAS). This procedure gives the corrected slant TEC. As slant TEC is dependent upon the ray path geometry through the ionosphere, it is required to calculate an equivalent vertical value of TEC which is independent of the elevation of the ray path. The vertical TEC is obtained by applying a mapping function "*m*" to slant TEC measurements. The mapping function is defined by [*Mannucci et al.*, 1993; *Langley et al.*, 2002] as

$$m = \frac{S\mathrm{TEC}}{V\mathrm{TEC}} = \frac{1}{\cos(\alpha)} \quad \text{or}$$

$$m = \frac{1}{\sqrt{1 - \sin^2\alpha}} = \frac{1}{\sqrt{1 - \left(\frac{R_{\mathrm{EARTH}}}{R_{\mathrm{EARTH}} + h_m}\cos(E)\right)^2}},$$

where E is the elevation angle of the satellite in degrees; m is the mapping function with zenith angle α at the ionospheric pierce point; R_{Earth} is the mean radius of the Earth in km and h_m is the ionosphere height above the Earth's surface. The height of the ionospheric pierce point is 300 km for the present study.

[10] The vertical TEC data thus obtained is further processed for each of the satellite passes with an elevation mask angle greater than 40° in order to avoid the effects of low elevation angles, such as tropospheric, water vapor scattering, and multi path effects. Therefore, the TEC observations are restricted to a latitude grid of ±3° and longitude grid of ±3° from the observing sites. The vertical TEC thus calculated is used when deriving the results presented in the following sections of this paper.

4. Background Space Weather Conditions

[11] The ionosphere is affected by many influences connected with solar and geomagnetic activities and sometimes from sources in the atmosphere or from below. In addition, ionospheric parameters vary with time of day, season, latitude, and longitude, as well as solar and magnetic activity conditions. Therefore, good knowledge of background ionospheric conditions is essential to extract the variations linked with seismic activities. Figures 2a–2c, illustrate the solar wind speed (*Vsw*), interplanetary magnetic field *Bz* component in GSM coordinates, and daily value of *Ap* index during 13–24 March 2008, 4–6 May 2008, and 19–29 August 2008. From those figures it is noted that solar and geomagnetic conditions during those periods were normally quiet and there was no major space weather

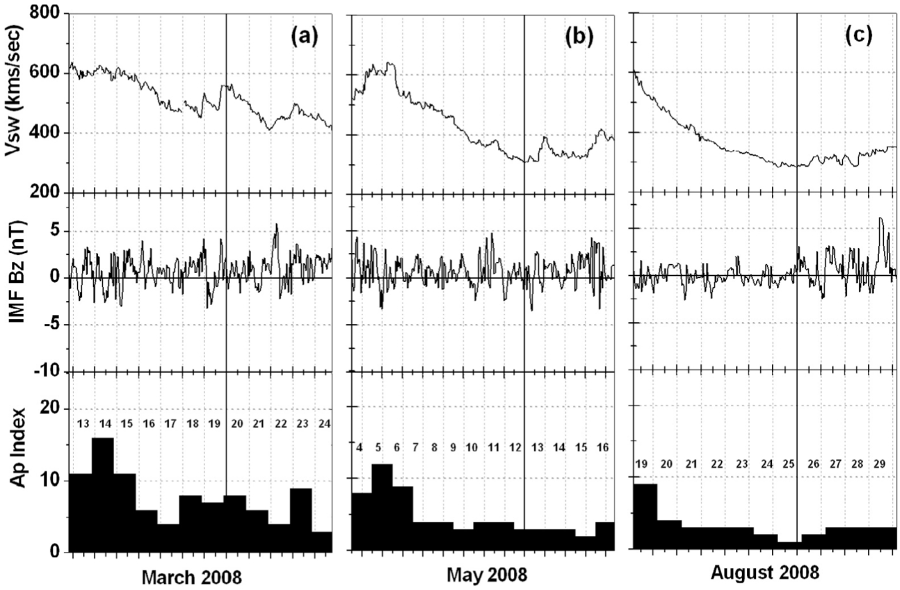

Figure 2. (a) Variation of solar wind bulk speed, interplanetary magnetic field (IMF) *Bz* measured from ACE satellite, and daily *Ap* indices on 13–24 March 2008. The vertical black line indicates the time of main shock of earthquake. (b) Same as Figure 2a, but for 4–16 May 2008. (c) Same as Figure 2a, but for 19–29 August 2008.

event observed during the period of any of the three major earthquakes. Based on the above space weather conditions, the anomalous ionospheric variations are examined for each earthquake by comparing the average distribution of foF_2 and TEC along latitude, longitude, and time for periods before and after the main shock of each earthquake. The three observing sites lie within the equatorial and low-latitude ionosphere, which is known for its highly dynamical nature as temporal and spatial changes in ionospheric para-

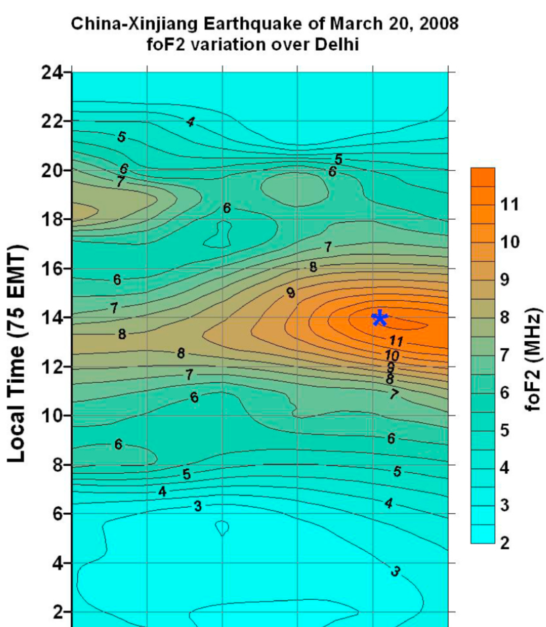

Figure 3a. Contour plots showing day-to-day variability of foF_2 over Delhi from 15–20 March 2008, five days prior to main shock of Xinjiang-Xizang earthquake of 20 March 2008. Blue star indicates the main precursor for this earthquake.

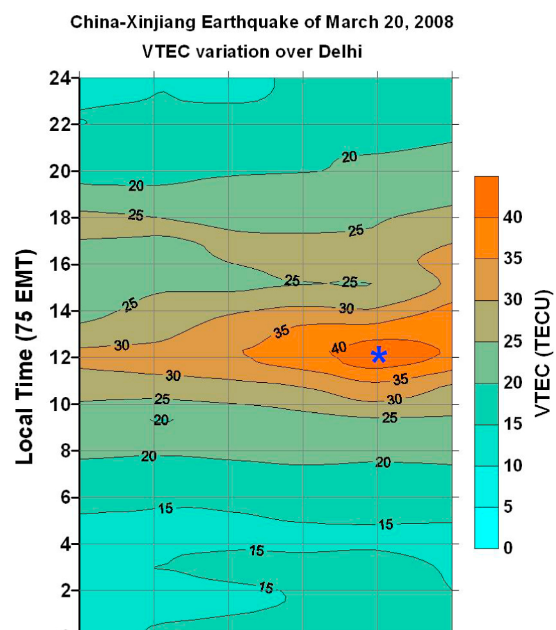

Figure 3b. Contour plots showing day-to-day variability of *V*TEC over Delhi from 15–20 March 2008, five days prior to main shock of Xinjiang-Xizang earthquake of 20 March 2008. Blue star indicates the main precursor for this earthquake.

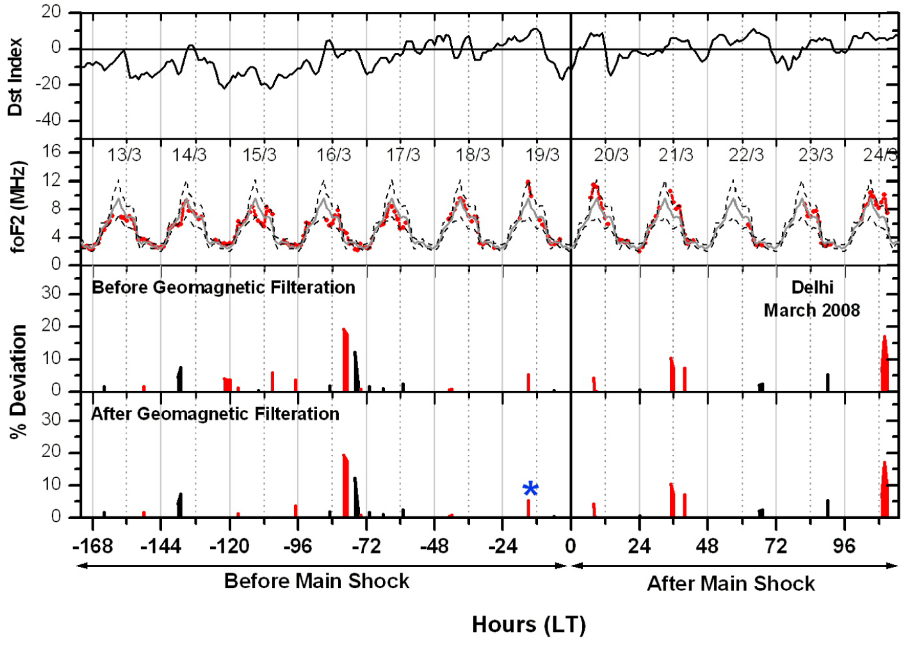

Figure 3c. From top to bottom are foF_2 (red line with dots) and *Dst* indices observed by the Delhi ionosonde during 13–24 March 2008. In the middle panel, red bars show percentage deviation of foF_2 from the upper bound of the interquartile range (IQR) and black bars show the percentage deviation from the lower bound of IQR. Percentage deviation is observed when the *Dst* index value is within ±15. The vertical black line shows the time of occurrence of the main shock of the earthquake. Blue star indicates the main precursor for this earthquake.

meters are significant at these latitudes, particularly during daytime, with maximum variations at equatorial ionization anomaly (EIA) crest regions. Thus, the latitudinal distribution of plasma associated with the EIA controls the day-to-day variability in ionospheric parameters in the Indian region. Furthermore, the hourly *Dst* index data is used and an arbitrary threshold value of ±15 nT is used to check whether the

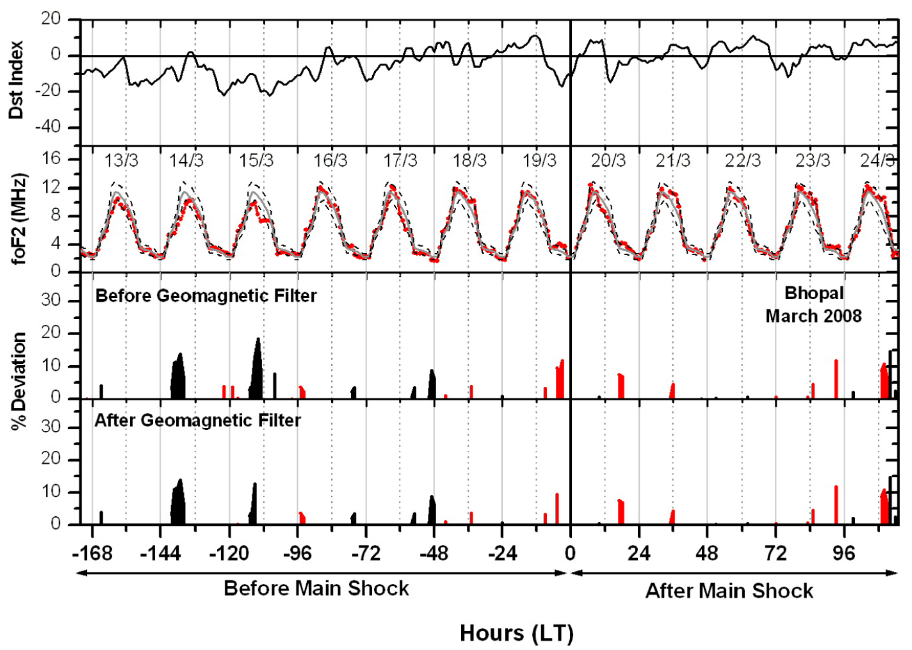

Figure 3d. Same as Figure 3c, but for Bhopal ionosonde observations.

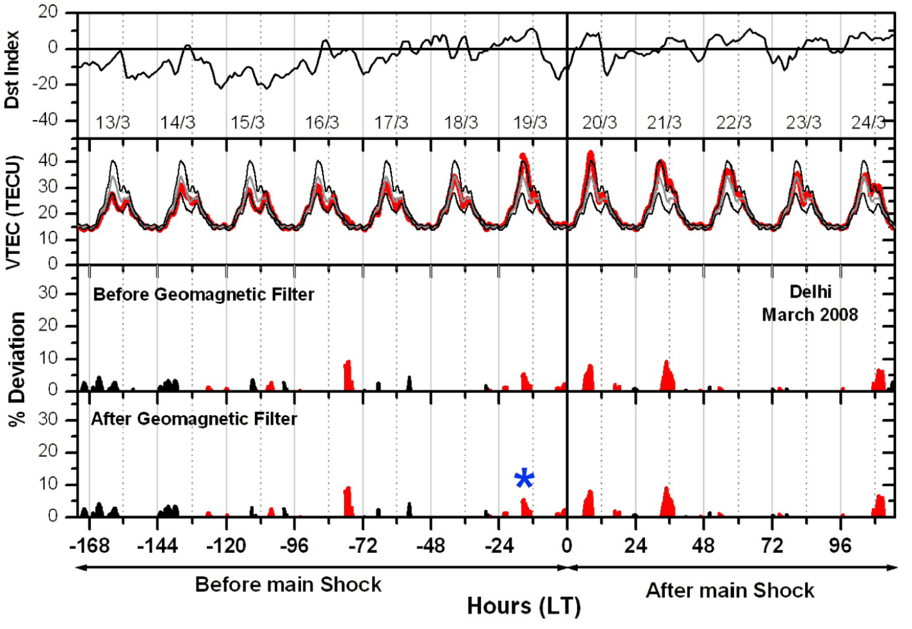

Figure 3e. Same as Figure 3c, but for GPS TEC recorded by the Delhi GPS receiver.

anomalous ionospheric variations are observed under quiet geomagnetic conditions.

5. Observations

5.1. Xinjiang-Xizang Border Region Earthquake of 20 March 2008

[12] On 20 March 2008, an immense earthquake ($M = 7.2$) struck the Xinjiang-Xizang border region of China at 0403 LT (see Table 1). Figures 3a and 3b show the contour plots of the diurnal variation of foF_2 and GPS TEC, respectively, from 15–20 March 2008 over Delhi, that is, up to 5 days prior to the main shock. These figures give a snapshot picture of foF_2 and TEC distribution over Delhi and clearly indicate an enhancement in both foF_2 and TEC on 19 March during the afternoon hours before the main shock. For detailed analysis, the variability of foF_2 and TEC a few days before and after the main shock of the earthquake are examined statistically following the method of *Liu et al.* [2004] with the results shown in Figures 3c–3f. Figures 3c and 3d show the day-to-day variations in foF_2, (red line with dots) along with the monthly median (solid shaded line) recorded from the Delhi and Bhopal ionosondes, respectively, during 13–24 March 2008. The ionosonde data of

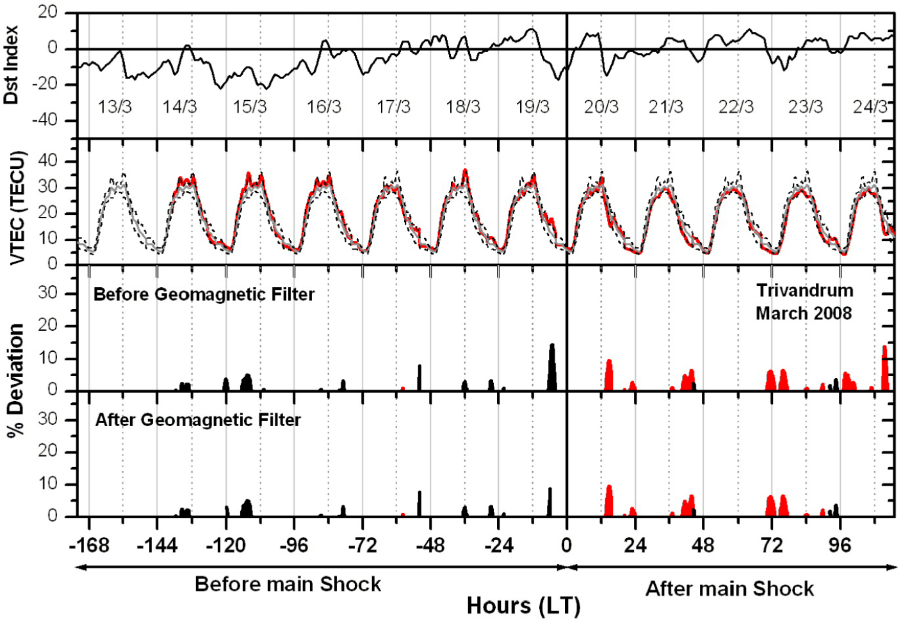

Figure 3f. Same as Figure 3c, but for GPS TEC recorded by the Trivandrum GPS receiver.

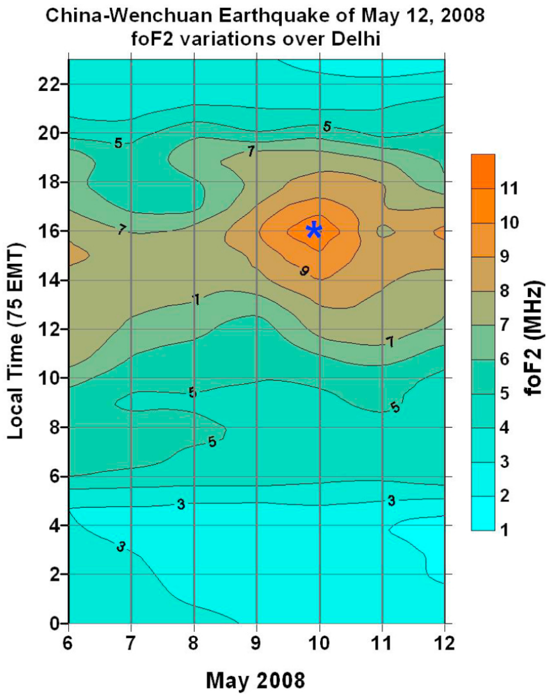

Figure 4a. Contour plots showing day-to-day variability of foF_2 over Delhi from 6–12 May 2008, six days prior to the main shock of the Wenchuan earthquake of 12 May 2008. Blue star indicates the main precursor for this earthquake.

both stations are analyzed using equations (1)–(4) and the results are shown in middle and bottom panels of Figures 3c and 3d along with hourly *Dst* values in the topmost panel. The middle panel in Figures 3c and 3d presents the deviations of foF_2 from the upper and lower bounds of IQR in red and black, respectively. The bottom panel shows the anomalous variations in foF_2 after filtering that associated with the geomagnetic disturbances with *Dst*±15 nT. The "0" hour represents the time of the main shock. From those figures it is noted that with respect to upper and lower bounds of IQR, both enhancement and depletion of foF_2 can be seen from 13–24 March on several intervals at both stations, and those changes have no correlation with known solar and geomagnetic conditions. It should be pointed out that Figure 3c shows anomalous enhancement of foF_2 over Delhi on the geomagnetic quiet day of 16 March. On 16 March, 78 hours before the main shock, the foF_2 in post-sunset hours (LT) at station Delhi increased ~20% from the upper bound, more than 1.3 times the median value. On 19 March, the foF_2 also shows an enhancement of ~5% from the upper bound during noon LT. If Figure 3c is compared with Figure 3a, it is found that the anomalous enhancement in foF_2 observed on 19 March over Delhi in Figure 3c is consistent with that of Figure 3a. However, at Bhopal, the increase in foF_2 was not as significant as over Delhi as is visible in Figure 3d; thus, indicating that this enhancement was a local phenomenon and not related with equatorial physical processes.

[13] To further confirm this feature, ionospheric TEC data of GPS receivers installed at Delhi and Trivandrum were used to derive the temporal variation of TEC and are plotted in Figures 3e and 3f in the same manner as in Figure 3c. The top panel of Figure 3e shows the temporal variation of *V*TEC (red line with dots) along with its monthly median (shaded line) from 13–24 March 2008 as observed over Delhi and Trivandrum. It is evident from the bottom panel of Figure 3e, that the GPS TEC shows abrupt variations during post-sunset hours (LT) on 16 and 19 March and also crosses the IQR upper bound by ~10% and ~5%, respectively, in geomagnetic quiet conditions over Delhi, whereas no such variations can be seen in *V*TEC observed over Trivandrum (as can be seen in Figure 3f) except when *V*TEC at Trivandrum crosses the IQR lower bound ~5 hours before the main shock. Close examination of Figure 3d reveals that simultaneous enhancement appeared in foF_2 at Bhopal ~4 hours before the main shock of the earthquake. Again, comparison between Figures 3e and 3b clearly confirms the anomalous enhancement in *V*TEC over Delhi on 19 March.

[14] The above observations of foF_2 and TEC clearly reveal that both ionospheric parameters showed large increase at Delhi, but not over Bhopal and Trivandrum. The anomalous enhancement observed on 19 March (a day before the main shock) during 1300–1500 LT may be considered as the main precursor of the Xinjiang-Xizang border region earthquake (period marked with a blue star in Figures 3a–3c, and 3e). The observations of foF_2 and TEC over Bhopal and Trivandrum suggest that the abnormal increase of ionospheric electron content and foF_2 was localized. The depletion observed 5 hours before the main shock at Trivandrum, followed by an increase in foF_2 at Bhopal after 1 hour, suggests its linkage with equatorial processes. The above results suggest that the localized strong ionospheric perturbations starting from around 78 hours before the main shock, under very quiet geomagnetic conditions, seem to be related to the earthquake.

5.2. Wenchuan County Earthquake of 12 May 2008

[15] A devastating earthquake (M = 8) hit Wenchuan County in southwest China on 12 May 2008. The contour diagrams of the diurnal variation of foF_2 and GPS TEC over Delhi from 6–12 May 2008, up to 6 days prior to the main shock, are presented in Figures 4a and 4b, respectively. These figures show a snapshot picture of foF_2 and TEC distribution over Delhi that clearly indicate an enhancement in both foF_2 and TEC on 10 May during the afternoon hours (LT) before the main shock. Again, the behavior of ionospheric parameters is analyzed statistically by excluding geomagnetic variability before and after the main shock of earthquake. To filter out the effects of $E \times B$ drifts on the Delhi ionosphere, the top panels in Figures 4c–4e show the day-to-day variations in foF_2, (red line with dots) along with its monthly median (solid shaded line) obtained from Delhi, Bhopal, and Trivandrum ionosondes, respectively, during 4–16 May 2008. The ionosonde data of all stations are analyzed using equations (1)–(4) and the results are shown in the middle and bottom panels of Figures 4c–4e along with hourly *Dst* values in the topmost panels. The middle panel in each figure represents the deviations of foF_2 from upper and lower bounds of IQR in red and black bars, respectively. The bottom panel shows the anomalous variations in foF_2 after filtering the one associated with geomagnetic disturbances with *Dst* ±15 nT. The "0" hour represents the time

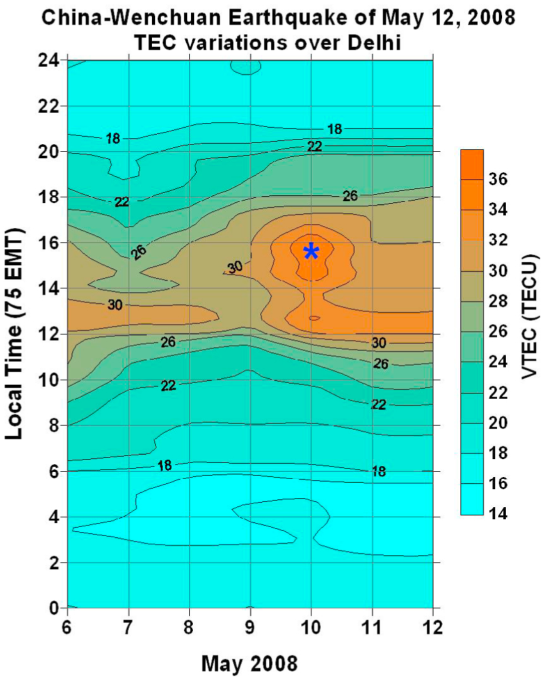

Figure 4b. Contour plots showing day-to-day variability of *V*TEC over Delhi from 6–12 May 2008, six days prior to main shock of the Wenchuan earthquake of 12 May 2008. Blue star indicates the main precursor for this earthquake.

of the main shock. From Figure 4c it is noted that, with respect to upper and lower bounds of IQR, both enhancement and depletion of foF_2, which have no correlation with the known solar and geomagnetic conditions, can be seen from 4–16 May on several intervals at Delhi. After filtering the disturbed ionospheric conditions, the most striking features in Figure 4c are the anomalous depletion and enhancement of foF_2 at 72 (9 May), 44 (10 May), and 11 (12 May) hours before the main shock. The critical frequency of the F_2 layer depleted by 9% from the IQR lower bound on 9 May and a strong depletion of 26% during pre-sunrise hours (LT), 10 hours before the main shock (Figure 4c). Apart from this, anomalous ionospheric variations of up to ~9% from the upper bound of IQR are observed about 44 hours (10 May) before the main shock of the Wenchuan earthquake. A comparison between Figures 4c and 4a clearly confirms the abnormal increase in ionospheric foF_2 over Delhi on 10 May. The ionospheric variability at Bhopal, which also lies within the earthquake preparation zone for this earthquake, shows enhancement of almost same magnitude from the upper bound of IQR after a time lag of one hour (Figure 4d). Other abnormal enhancements over Bhopal are observed 30 hours (15%) and 17 hours (8%) before the main shock of the earthquake and occur under very quiet geomagnetic conditions. However, at Trivandrum, an equatorial station lying outside the earthquake preparation zone, the variability in foF_2 did not show any significant variation as was observed over Delhi and Bhopal (see Figure 4e). The above observations of foF_2 over the three Indian ionospheric stations, which encompass

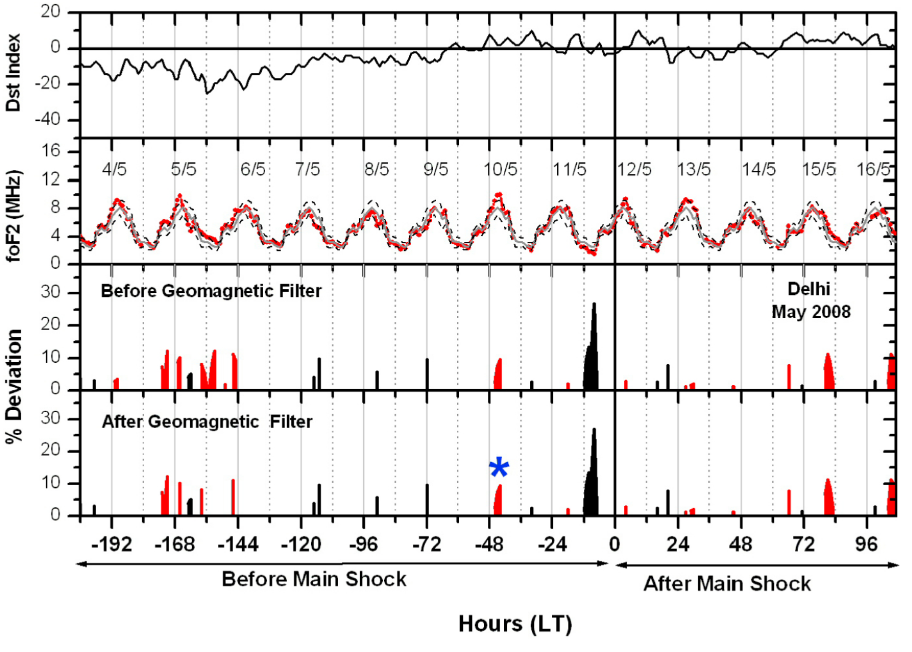

Figure 4c. From top to bottom are foF_2 (red line with dots) and *Dst* indices observed by the Delhi ionosonde during 4–16 May 2008. In the middle panel, red bars show percentage deviation of foF_2 from the upper bound of IQR and black bars show the percentage deviation from the lower bound of IQR. Percentage deviation is observed when *Dst* index value is within ±15. The black line shows the time of occurrence of the main shock of the earthquake. Blue star indicates the main precursor for this earthquake.

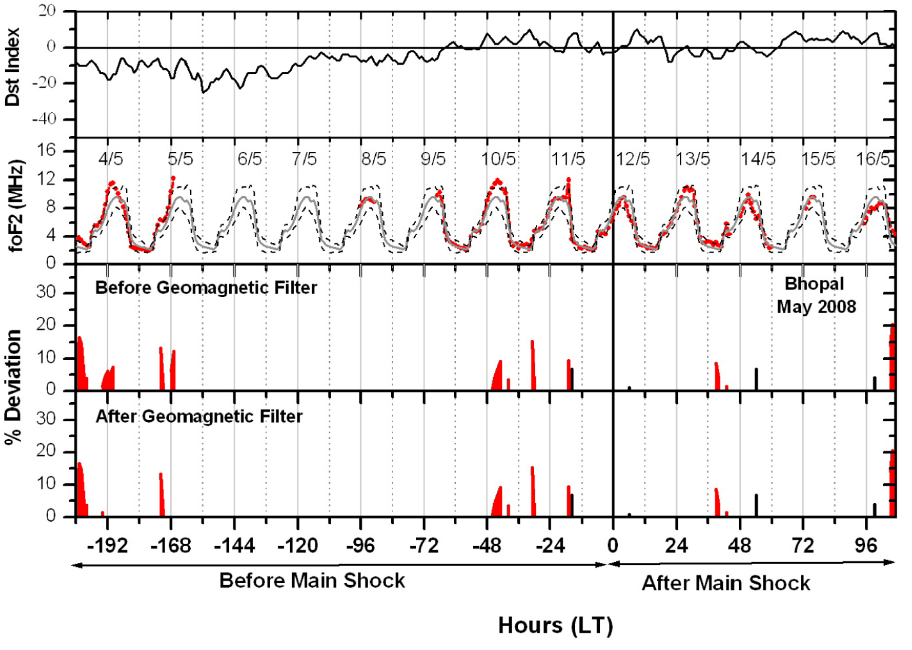

Figure 4d. Same as Figure 4c, but for Bhopal ionosonde observations.

equatorial and low latitude ionospheres, clearly indicate that the enhancement and depletion of ionization was not controlled by equatorial physical processes of ionization distribution, rather it might be due to some other source from a northward direction. If the ionization variation was controlled by the equatorial processes, it would appear first at Bhopal and, after a time lag of 1–2 hours, at Delhi.

[16] For the further confirmation of these anomalous features, ionospheric TEC data of GPS receivers installed at Delhi and Trivandrum were used to derive the temporal variation of TEC that is plotted in Figures 4f and 4g for the same periods as those in Figures 4c–4e. The similar methodology has been adopted to Figures 4f and 4g as Figures 4c, 4d, and 4e. It is evident from the bottom panel of Figure 4f that the GPS TEC also shows similar abrupt variations under very quiet geomagnetic conditions in the form of enhancements and depletions of TEC at various time intervals, for example, 168 (17%), 115 (5%), 72 (4%), 44 (~25%) and 11 (16%) hours before the main shock, as was observed in foF_2 over Delhi. The anomalous enhance-

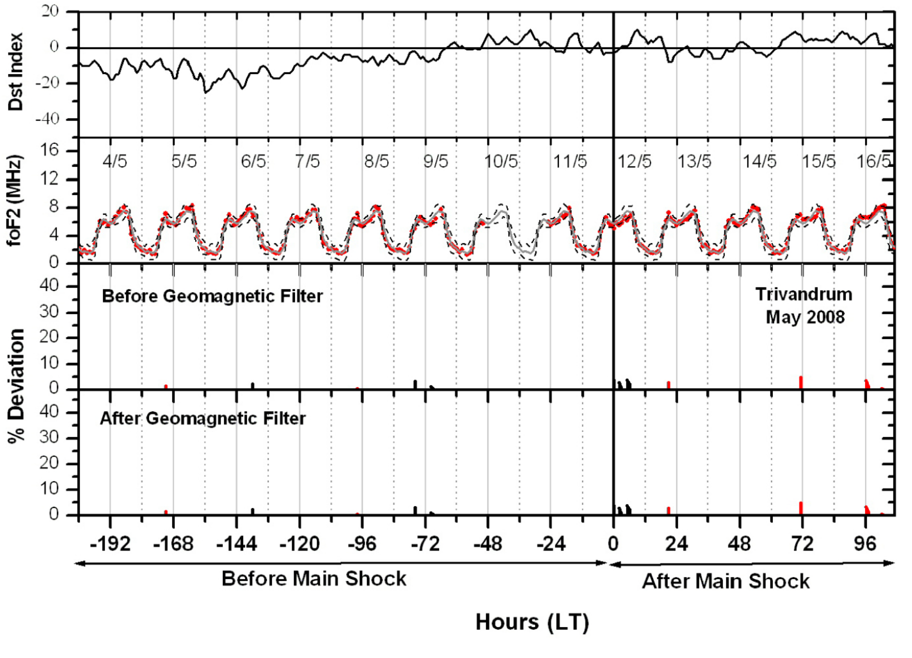

Figure 4e. Same as Figure 4c, but for Trivandrum ionosonde observations.

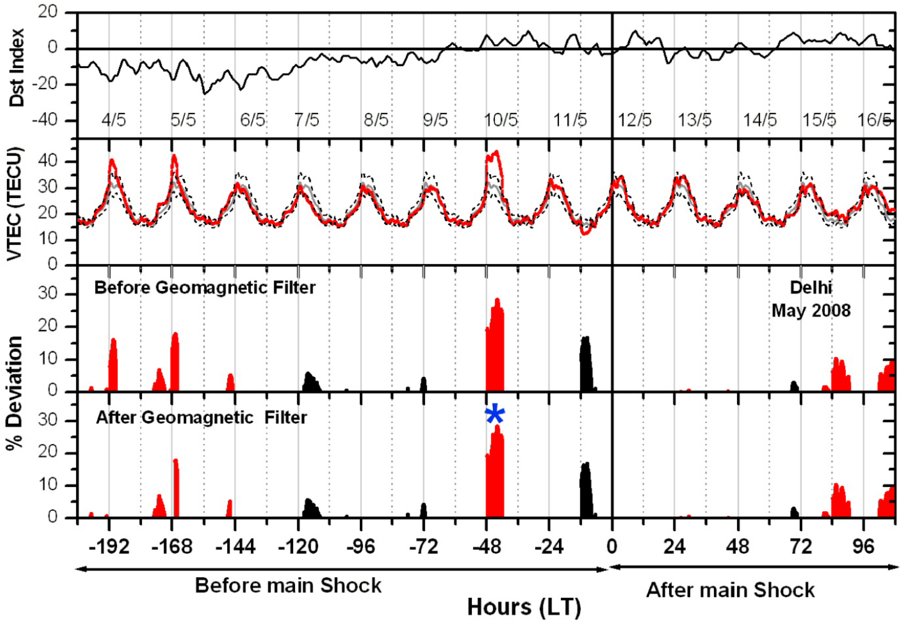

Figure 4f. Same as Figure 4c, but for GPS TEC recorded by the Delhi GPS receiver.

ment in TEC from the upper bound of IQR on 10 May during noon hours (LT) and simultaneous depletion from the lower bound of IQR on 11 May during the pre-sunrise hours (LT) is significant and confirms the unusual behavior of foF_2 observed at Delhi. Again, a comparison of Figures 4f and 4b confirms the abnormal increase in GPS TEC over Delhi on 10 May, likewise for ionospheric foF_2. Figure 4g demonstrates the TEC variation over Trivandrum during the same period. It can be seen from Figure 4g that there are no anomalous variations of TEC at this equatorial station; thus, confirming the observations of foF_2.

[17] Both the observations of foF_2 and TEC clearly indicate abnormal enhancements and depletions of ionospheric plasma several hours before the main shock of the Wenchuan County earthquake occurred over the Delhi and Bhopal ionospheric stations (both stations are within the earthquake preparation zone) but not over the third Indian ionospheric station, Trivandrum. The significant ionospheric perturbations observed in foF_2 and TEC under quiet solar geophysical

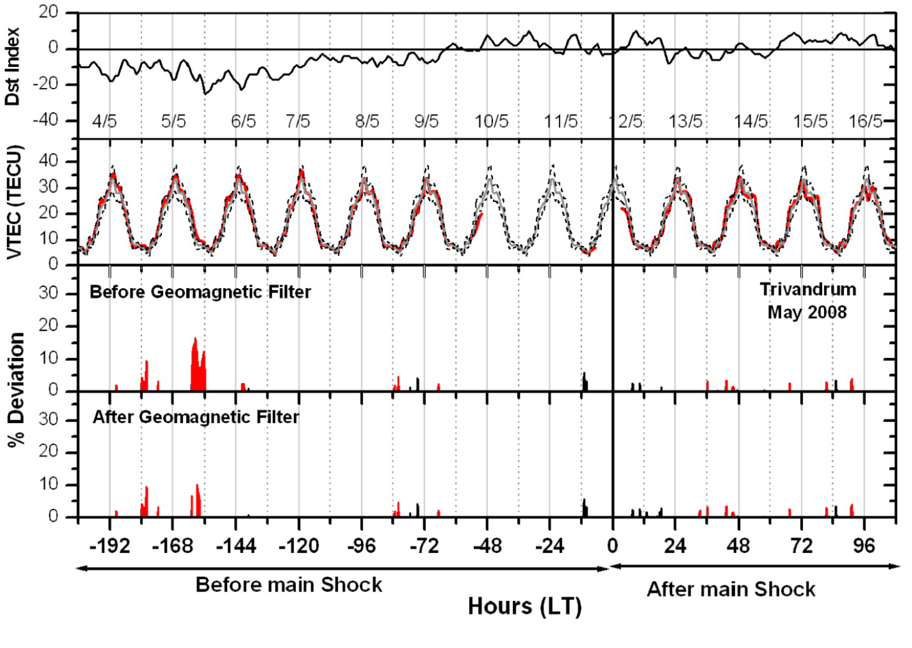

Figure 4g. Same as Figure 4c, but for GPS TEC recorded by the Trivandrum GPS receiver.

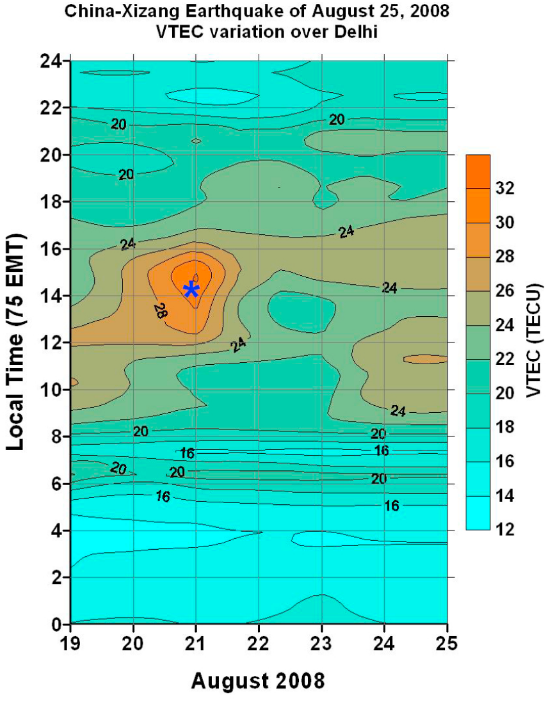

Figure 5a. Contour plots showing day-to-day variability of *V*TEC over Delhi from 19–25 August 2008, six days prior to the main shock of the western Xizang earthquake of 25 August 2008. Blue star indicates the main precursor for this earthquake.

conditions (1400–1700 LT) around 2 days before the main shock (i.e., 10 May) over Delhi and Bhopal may be considered as the main precursor of this deadly earthquake (marked with a blue star in Figures 4a–4c and 4f).

5.3. Western Xizang Earthquake of 25 August 2008

[18] On 25August 2008, an earthquake ($M = 6.7$) occurred in the western Xizang region of China. Figure 5a shows the contour diagram of the diurnal variation of GPS TEC over Delhi from 19–25 August 2008, that is, up to 6 days prior to the main shock. It may be seen from these figures that the diurnal maximum in TEC (~28 TEC*U*) occurs approximately between 1200 and 1400 LT at Delhi. The day maximum values of TEC show abrupt enhancement on 21 August and attain a value of 32 TEC*U* at 1500 LT. As earlier, the observed anomalous behaviors of ionospheric parameters (foF_2 and TEC) a few days before and after the main shock are plotted in Figures 5b–5d. For this earthquake, the GPS TEC data of Delhi and Trivandrum and the ionosonde data of Bhopal are plotted in Figures 5b, 5c, and 5d, respectively, using the same pattern as in Figures 3 and 4. Figures 5b and 5d show the temporal variation of *VTEC* (red line with dots) as recorded by the Delhi and Trivandrum GPS receivers, respectively, during 19–29 August 2008 and Figure 5c shows the temporal variation of foF_2 (red line with dots) derived from the Bhopal ionosonde for the same period along with the monthly median (shaded line). Close examination of Figure 5b reveals noticeable enhancement and depletion of TEC before the main shock during several

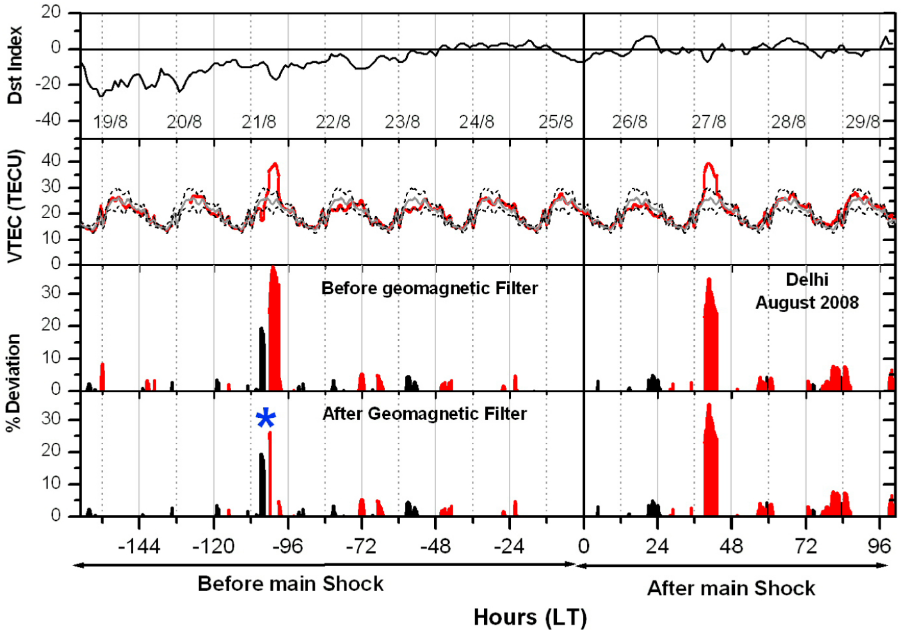

Figure 5b. From top to bottom are *V*TEC (red line with dots) and *Dst* indices observed by the Delhi GPS receiver during 19–29 August 2008. In the bottom panels, red bars show percentage deviation of *V*TEC from the upper bound of IQR and black bars show the percentage deviation from the lower bound of IQR. Percentage deviation is observed when *Dst* index value is within ±15. The black line shows the time of occurrence of the main shock of the earthquake. Blue star indicates the main precursor for this earthquake.

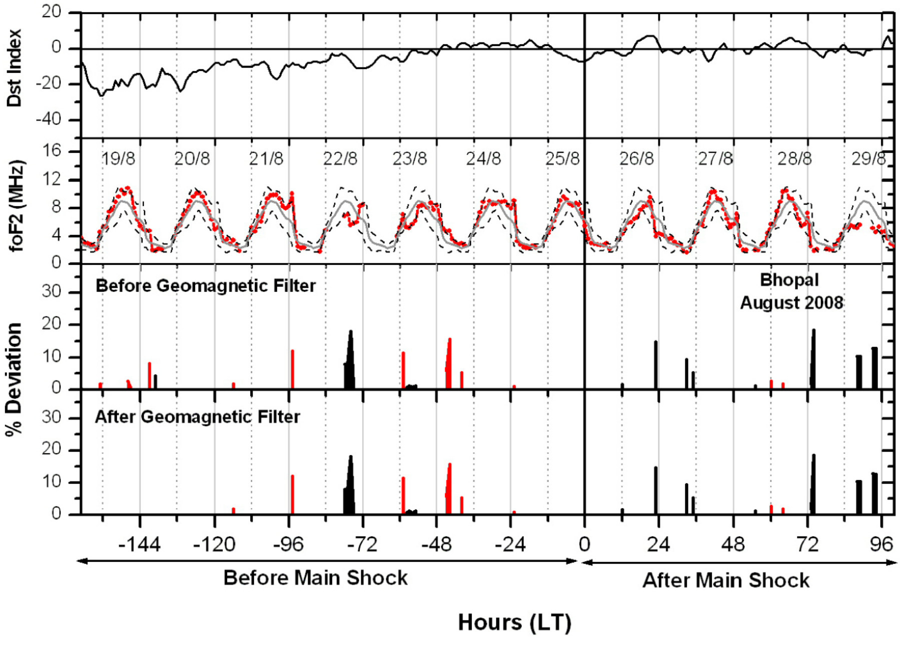

Figure 5c. Same as Figure 5b, but for Bhopal ionosonde observations.

intervals at Delhi, of which the prominent ones are at 104 (19% from the IQR lower bound) and 100 (37% from the IQR upper bound) hours before the main shock. It should be pointed out that the most striking feature in Figure 5b is the strong enhancement of TEC over Delhi on the geomagnetic quiet day, 21 August. This strong enhancement in TEC appeared at Delhi and at Bhopal ~100 hours before the main shock. Simultaneous enhancements of ~15% from the upper bound of IQR in foF_2 are evident in Figure 5c after 4 hours, that is, at 96 hours before the main shock. However, no such enhancement or depletion of ionospheric plasma is observed at Trivandrum (see Figure 5d).

[19] A comparison between contour and diurnal plots of GPS TEC, shown in Figures 5a and 5b, respectively, confirms the anomalous enhancement in the ionospheric plasma over Delhi during 1400–1600 LT on 21 August, 3 days before the main shock of the western Xizang earthquake and may be considered as a main precursor of that earthquake (period marked with a blue star in Figures 5a and 5b). The observations of Bhopal and Trivandrum suggest that this

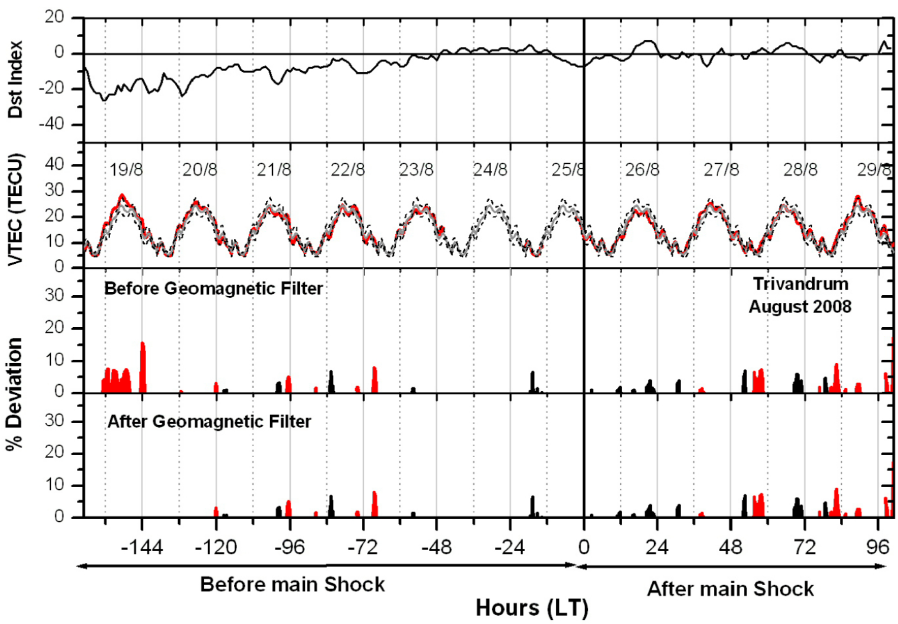

Figure 5d. Same as Figure 5b, but for Trivandrum GPS TEC observations.

enhancement of ionospheric plasma over Delhi is localized in nature.

6. Discussion and Conclusion

[20] In the present study, to determine linkages between the abnormal ionospheric variations and the earthquakes, a statistical analysis of ionosonde and GPS TEC data from three Indian stations, which encompass the equatorial and low-latitude ionosphere, is carried out during the periods of three recent major 2008 seismic events in China. In the equatorial and low-latitude ionosphere, the maximum electron density occurs at EIA crest regions inspite at the equator due to fountain effect. The diurnal variation in ionospheric parameters at the EIA region shows a steep increase and reaches a maximum value between 1300 and 1600 LT, while at the equator the peak is broad and occurs around 1600 LT. A short-lived day minimum occurs between 0500 and 0600 LT at all stations from the equator to the EIA crest region. Beyond the crest region, the day maximum values decrease with an increase in latitude [*Rama Rao et al.*, 2006]. Also on a short-term basis (i.e., day-to-day or hour-to-hour) the Earth's ionosphere is strongly dependent on magnetic disturbances originating from the Sun and the equatorial electric field plays an important role in the distribution of plasma over the equatorial and low-latitude F_2 layer ionosphere under both quiet and active geomagnetic conditions. Magnetic disturbances destabilize the equatorial electric field, which in turn affects the distribution of plasma in the equatorial and low-latitude ionosphere. The perturbations in the equatorial plasma drift are due to the combined effects of direct penetration electric fields and longer lasting ionospheric disturbed dynamo electric fields. Prompt penetration electric fields occur during periods of rapid and large interplanetary magnetic field (IMF) changes. Therefore, solar wind and magnetospheric driving mechanisms often directly affect the equatorial and low-latitude ionosphere [*Huang et al.*, 2005; *Tsurutani et al.*, 2004; *Zhao et al.*, 2005]. It is evident from Figures 2a–2c that the IMF *Bz* ranges from −5.6 to 5.8 nT, *Ap* index varies from 2 to 23, *Dst* index varies from −28 to 11 nT, and the solar wind speed ranges from 284.3 to 643.2 km/s during the three seismic activity periods. This clearly indicates that the solar geophysical conditions were mostly at quiet to normal levels around the time of these earthquakes. Moreover, the observations of foF_2 and TEC over the equatorial station Trivandrum and the EIA crest station Bhopal clearly do not support any possibility of modification in the equatorial electric field. Hence, the observed unusual variations in ionospheric parameters over Delhi cannot be correlated with the geomagnetic conditions and do not indicate their linkage with equatorial processes. Sometimes, day-to-day variability of the ionosphere may be caused by sources from the lower atmosphere such as planetary waves [*Altadill and Apostolov*, 2003; *Xiong et al.*, 2006]. However, planetary waves cannot propagate directly upward to the altitude of the F_2 layer, due to the viscosity effects, but they can affect *F* region processes via modulating ionospheric *E* layer dynamo electric fields with mapping to higher altitudes along geomagnetic field lines. Therefore, if there are any unusual variations in the ionosphere observed under quiet other possible conditions, then one may try to look for another source, like a seismic event. The observations of the present study also report unusual enhancements and depletions of ionospheric foF_2 and TEC values, observed over Delhi 1–4 days before the main shock of each seismic event, with Delhi being the nearest of the three Indian stations to the epicenter of earthquakes. The anomalies suggest a possible linkage with seismic activities. The main identified precursors for the three seismic events were observed during daytime. As solar activities were at very low levels during 2008, the EIA crest would be confined to much lower latitudes and cannot reach the Delhi latitude; hence, the unusual enhancements observed over Delhi, other than those related to magnetic disturbances or of equatorial origin, can be considered of local origin and may be related to seismic activities.

[21] *Zhao et al.* [2008] by using data from a chain of six ionosondes reported that abnormal enhancement 3 days (9 May 2008) before the main shock (12 May) of the Wenchuan earthquake was confined mainly to 90°E–130°E longitudes. For this earthquake, similar results were reported by *Liu et al.* [2009] using GPS TEC data. Therefore, in the Wenchuan earthquake there was no such enhancement in foF_2 and GPS-TEC observed in western longitudes to the epicenter like Delhi. *Pulinets et al.* [2006] reported that the anomalous increment of *VTEC* appeared 2 and 3 days before the $M = 7.8$ Colima earthquake of 21 January 2003 in which the maximum anomalous enhancement was beyond 50% relative to the monthly mean.

[22] The one possibility for these pre-earthquake ionospheric anomalies could be strong atmospheric electric fields generated on, or near, the ground surface during pre-seismic periods. Such an atmospheric electric field may be caused by ions generated from radon emissions. The increased radon emanation from active faults and cracks before earthquakes can ionize the near ground atmosphere producing a large vertical electric field at the earth's surface [*Pulinets and Boyarchuk*, 2004]. It was also pointed out by *Freund* [2000] that positively charged holes, associated with microfracturing prior to earthquakes, diffuse from the focal zone to the ground surface. Through a quasi-electrostatic model of atmosphere-thermosphere-ionosphere coupling, *Kim and Hegai* [1999] and *Pulinets et al.* [2000] showed that a strong vertical electric field on the Earth's surface could penetrate into the ionosphere and modify its dynamics and electron density distribution prior to the earthquake onset. Their results estimated that a vertical electric field of ~1 kV/m at the ground surface can produce a horizontal electric field of ~1 mV/m at ionospheric heights.

[23] The present study focused only on demonstrating the ionospheric variability characteristics before the main shock of seismic events. In conclusion, the anomalous enhancement of the ionospheric foF_2 and TEC over Delhi 1–4 days prior to three strong earthquakes of China was unique. In the view of the near Earth–space environment, it was unlikely to be caused by geomagnetic activities. The spatial distribution of the anomalies was very local, which probably indicates association with seismoionospheric coupling processes. However, for elucidation of this kind of seismoionospheric effect, further investigation is required.

[24] **Acknowledgments.** One of the authors (Dr. Kavita Sharma) would like to thank the Council of Scientific and Industrial Research (CSIR) India for providing Research Associate financial support.

[25] Zuyin Pu thanks the reviewers for their assistance in evaluating this manuscript.

References

Altadill, D., and E. M. Apostolov (2003), Time and scale size of planetary wave signatures in the ionospheric *F* region: Role of the geomagnetic activity and mesosphere/lower thermosphere winds, *J. Geophys. Res.*, *108*(A11), 1403, doi:10.1029/2003JA010015.

Chuo, Y. J., J. Y. Liu, S. A. Pulinets, and Y. I. Chen (2002), The ionospheric perturbations prior to the Chi-Chi and Chia-Yi earthquakes, *J. Geodyn.*, *33*, 509–517.

Dabas, R. S., R. M. Das, K. Sharma, and K. G. M. Pillai (2007), Ionospheric pre-cursors observed over low latitudes during some of the recent major earthquakes, *J. Atmos. Sol. Terr. Phys.*, *69*, 1813–1824, doi:10.1016/j.jastp.2007.09.005.

Dobrovolsky, I. R., S. I. Zubkov, and V. I. Myachkin (1979), Estimation of the size of earthquake preparation zones, *Pure Appl. Geophys.*, *117*, 1025–1044.

Dutta, H. N., R. S. Dabas, R. M. Das, K. Sharma, B. K. Singh (2007), Ionospheric perturbations over Delhi caused by the 26 December 2004 Sumatra Earthquake, *Int. J. Remote Sens.*, *28*, 3141–3151, doi:10.1080/01431160601099590.

Freund, F. (2000), Time-resolved study of charge generation and propagation in igneous rocks, *J. Geophys. Res.*, *105*, 11,001–11,019, doi:10.1029/1999JB900423.

Gokhberg, M. B., V. A. Pilipenko, and O. A. Pokhotelov (1983), On the seismic precursors in the ionosphere, *Izv. Akad. Nauk SSSR, Ser. Fiz. Zemli*, *10*, 17–21.

Huang, C. S., J. C. Foster, and M. C. Kelley (2005), Long-duration penetration of the interplanetary electric field to the low-latitude ionosphere during the main phase of magnetic storms, *J. Geophys. Res.*, *110*, A11309, doi:10.1029/2005JA011202.

Ishkova, L. M., E. M. Kovalevskaya, and V. A. Morgunov (1994), Ionospheric disturbances during the Chile earthquake in May 1960, *Dokl. Akad. Nauk*, *334*, 500–506.

Kim, V. P., and V. V. Hegai (1999), A possible presage of strong earthquakes in the night-time mid-latitude F_2 region ionosphere, in *Atmospheric and Ionospheric Electromagnetic Phenomena Associated with Earthquakes*, pp. 619–627, Terra Sci., Tokyo, Japan.

Langley, R., M. Fedrizzi, E. Paula, M. Santos, and A. Komjathy (2002), Mapping the low latitude ionosphere with GPS, *GPS World*, *13*, 41–46.

Legen'ka, A. D., S. A. Pulinets, and S. D. Gregory (1995), Reaction of the ionosphere to the Italian earthquake of November 23, 1980, *Inst. Terr. Magn. Ionos. Radio Wave Propag.*, *12*, 1081–1087.

Liperovskaya, E. V., V. A. Liperovsky, A. S. Silina, and M. Parrot (2006), On spread-F in the ionosphere before earthquakes, *J. Atmos. Sol. Terr. Phys.*, *68*, 125–133, doi:10.1016/j.jastp.2005.10.005.

Liu, J. Y., Y. I. Chen, S. A. Pulinets, Y. B. Tsai, and Y. J. Chuo (2000), Seismoionospheric signatures prior to M ≥ 6.0 Taiwan earthquakes, *Geophys. Res. Lett.*, *27*, 3113–3116, doi:10.1029/2000GL011395.

Liu, J. Y., Y. I. Chen, Y. J. Chuo, and H. F. Tsai (2001), Variations of ionospheric total electron content during the Chi-Chi earthquake, *Geophys. Res. Lett.*, *28*, 1383–1386, doi:10.1029/2000GL012511.

Liu, J. Y., Y. J. Chuo, S. J. Shan, Y. B. Tsai, Y. I. Chen, S. A. Pulinets, and S. B. Yu (2004), Pre-earthquake ionospheric anomalies registered by continuous GPS TEC measurements, *Ann. Geophys.*, *22*, 1585–1593, doi:10.5194/angeo-22-1585-2004.

Liu, L., W. Wan, M.-L. Zhang, and B. Zhao (2008a), Case study on total electron content enhancements at low latitudes during low geomagnetic activities before the storms, *Ann. Geophys.*, *26*, 893–903, doi:10.5194/angeo-26-893-2008.

Liu, L., W. Wan, M.-L. Zhang, B. Zhao, and B. Ning (2008b), Prestorm enhancements in NmF_2 and total electron content at low latitudes, *J. Geophys. Res.*, *113*, A02311, doi:10.1029/2007JA012832.

Liu, J. Y., et al. (2009), Seismoionospheric GPS total electron content anomalies observed before the 12 May 2008 M_w7.9 Wenchuan earthquake, *J. Geophys. Res.*, *114*, A04320, doi:10.1029/2008JA013698.

Mannucci, A. J., B. D. Wilson, and C. D. Edwards (1993), A new method for monitoring the Earth's ionospheric total electron content using the GPS global network, *Proc. of ION GPS-93, Sixth Int. Tech. Meet., Satell. Div., Inst. Navig.*, *1993*, 1323–1332.

Ondoh, T., and M. Hayakawa (1999), Anomalous occurrence of sporadic-*E* layers before the Hyogoken-Nanbu earthquake, M7.2 of January 17, 1995, in *Atmospheric and Ionospheric Electromagnetic Phenomena*, edited by M. Hayakawa, pp. 629–639, Terra Sci., Tokyo, Japan.

Popov, K. V., V. A. Liperovsky, C.-V. Meister, P. F. Biagi, E. V. Liperovskaya, and A. S. Silina (2004), On ionospheric precursors of earthquakes in scales of 2–3 h, *Phys. Chem. Earth*, *29*, 529–535.

Pulinets, S. A., and A. D. Legen'ka (2003), Spatial-temporal characteristics of large scale distributions of electron density observed in the ionospheric *F*-region before strong earthquakes, *Cosmic Res.*, *41*, 221–229, doi:10.1023/A:1024046814173.

Pulinets, S. A., and K. A. Boyarchuk (2004), *Ionospheric Precursors of Earthquakes*, Springer, Berlin.

Pulinets, S. A., A. D. Legen'ka, and V. A. Alckseev (1994), Pre-earthquake ionospheric effects and their possible mechanisms, in *Dusty and Dirty Plasmas, Noise, and Chaos in Space and in the Laboratory*, edited by H. Kikuchi, pp. 545–557, Plenum, New York.

Pulinets, S. A., K. A. Boyarchuk, V. V. Hegai, V. P. Kim, and A. M. Lomonosov (2000), Quasielectrostatic model of atmosphere-thermosphere-ionosphere coupling, *Adv. Space Res.*, *26*, 1209–1218.

Pulinets, S. A., et al. (2006), Thermal, atmospheric and ionospheric anomalies around the time of the Colima M7.8 earthquake of 21 January 2003, *Ann. Geophys.*, *24*, 835–849, doi:10.5194/angeo-24-835-2006.

Rama Rao, P. V. S., S. Gopi Krishna, K. Niranjan, and D. S. V. V. D. Prasad (2006), Temporal and spatial variations in TEC using simultaneous measurements from the Indian GPS network of receivers during the low solar activity period of 2004–2005, *Ann. Geophys.*, *24*, 3279–3292, doi:10.5194/angeo-24-3279-2006.

Rishbeth, H., and M. Mendillo (2001), Patterns of ionospheric variability, *J. Atmos. Sol. Terr. Phys.*, *63*, 1661–1680.

Sharma, K., R. M. Das, R. S. Dabas, K. G. M. Pillai, S. C. Garg, and A. K. Mishra (2008), Ionospheric precursors observed at low latitudes around the time of Koyna Earthquake, *Adv. Space Res.*, *42*, 1238–1245, doi:10.1016/j.asr.2007.06.026.

Tsurutani, B., et al. (2004), Global dayside ionospheric uplift and enhancement associated with interplanetary electric fields, *J. Geophys. Res.*, *109*, A08302, doi:10.1029/2003JA010342.

Van Dierendonck, A. J., P. Fenton, and J. Klobuchar (1996), Commercial ionospheric scintillation monitoring receiver development and test results, *52nd Ann. Tech. Meet., Proc. Inst. Navig.*, *21*, 573–582.

Xiong, J., W. Wan, B. Ning, L. Liu, and Y. Gao (2006), Planetary wave-type oscillations in the ionosphere and their relationship to mesospheric/lower thermospheric and geomagnetic disturbances at Wuhan (30.61°N, 114.51°E), *J. Atmos. Sol. Terr. Phys.*, *68*, 498–508, doi:10.1016/j.jastp.2005.03.018.

Zelenova, T. I., and A. D. Legen'ka (1988), Ionospheric effects related to the Moneron earthquake of September 5–6, 1971, *Izv. Akad. Nauk SSSR, Ser. Fiz. Zemli*, *10*, 89–95.

Zelenova, T. I., V. V. Migulin, M. N. Fatkullin, A. D. Legen'ka, and Ts. Pashova (1991), Instability of the F_2 region prior to the Vranchesk earthquake on August 31, 1986, *Dokl. Acad. Nauk SSSR*, *317*, 620–625.

Zhao, B., W. Wan, and L. Liu (2005), Responses of equatorial anomaly to the October–November 2003 superstorms, *Ann. Geophys.*, *23*, 693–706.

Zhao, B., M. Wang, T. Yu, W. Wan, J. Lei, L. Liu, and B. Ning (2008), Is an unusual large enhancement of ionospheric electron density linked with the 2008 great Wenchuan earthquake?, *J. Geophys. Res.*, *113*, A11304, doi:10.1029/2008JA013613.

R. M. Das, R. S. Dabas, S. K. Sarkar, and K. Sharma, Radio and Atmospheric Sciences Division, National Physical Laboratory, Dr. K.S. Krishnan Marg, New Delhi, IN-110012, India. (sharmak@mail.nplindia.org)

A. K. Gwal, Institute of Physics and Electronics, Barkatullah University, Bhopal Hoshangabad Road, Bhopal, Madhya Pradesh, IN-462026, India.

S. Ravindran, Space Physics Laboratory, Vikram Sarabhai Space Center, Thiruvananthapuram, Trivandrum, Kerala, IN-695022, India.